

Raport stiintific

privind implementarea proiectului in perioada ianuarie – decembrie 2014

Activitatile desfasurate in perioada mentionata mai sus au vizat analiza datelor experimentale obtinute folosind aranjamentul experimental ALICE de la LHC-CERN in interactia p + p la energia de 7 TeV, dezvoltari fenomenologice si teoretice prezentate in cele ce urmeaza in limba engleza pentru o vizibilitate mai buna a paginii WEB a proiectului.

- *Light flavor hadron spectra at low p_T and search for collective phenomena in high multiplicity pp, p-Pb and Pb-Pb collisions measured with the ALICE experiment at $\sqrt{s} = 7$ TeV*

- Blast wave model fits and comparison with p-Pb and Pb-Pb collisions

As described in the 2013 report the ALICE Collaboration has recently presented detailed results, obtained by us, on transverse momentum spectra of π^+ , K^+ and p measured at LHC in pp collisions at $\sqrt{s} = 7$ TeV as a function of charged particle multiplicity [1]. The charged particle multiplicity was measured in the central pseudorapidity region $|\eta| \leq 0.8$ and the analysis was done in a narrower range of rapidity $|y| \leq 0.5$. The p_T spectra were analyzed from 0.2 GeV/c, 0.3 GeV/c and 0.5 GeV/c up to 2.6 GeV/c, 1.4 GeV/c and 2.6 GeV/c for π^+ , K^+ and p respectively and in eight bins of multiplicity up to ~ 50 measured charged particle multiplicity density per unit of pseudorapidity.

The p_T dependence of p/π for the second and highest multiplicity bins and of $(p + p)/(\pi^+ + \pi^-)$ ratio for p-Pb in 60–80% and 0–5% multiplicity classes and for Pb-Pb at 80–90% and 0–5% centralities [2] are presented in Fig. 1(a) and Fig. 1(b), respectively. The push of protons towards larger p_T values relative to pions with increasing centrality or multiplicity is present for all three systems. Quantitatively, this can be followed in Fig. 1(c) where the ratios of the ratios shown in Fig. 1(a) and Fig. 1(b) are presented. The ratio for pp follows closely the p-Pb trend as a function of p_T .

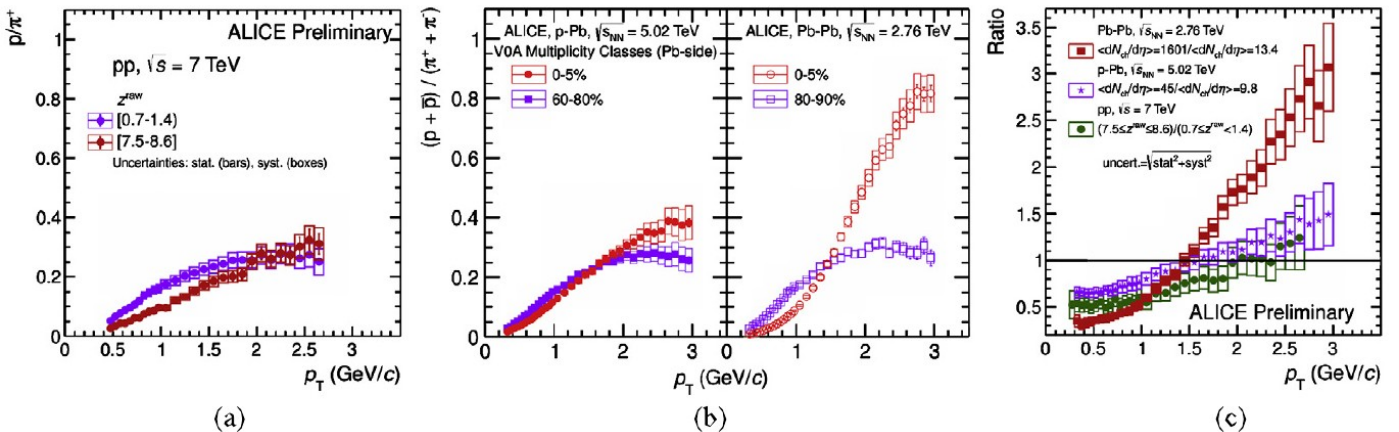


Fig. 1. (a) p_T dependence of p/π ratio for the second and highest multiplicity bins in pp collisions; (b) p_T dependence of $(p + p)/(\pi^+ + \pi^-)$ ratio in p-Pb for 60–80% and 0–5% multiplicity classes and Pb-Pb for 80–90% and 0–5% centralities [2]; (c) The ratios of the ratios presented in (a) and (b).

Based on these similarities, information on collective type dynamics from the fits of experimental transverse momentum spectra using expressions inspired by hydrodynamical models [3] was obtained. The average transverse expansion velocity and kinetic freeze-out temperature were obtained as parameters of the following expression used for the fit:

$$E \frac{d^3N}{dp^3} \sim f(p_i) = \int_0^R m_T K_1(m_T \cosh \rho / T_{fo}) I_0(p_T \sinh \rho / T_{fo}) r dr$$

where:

$$m_T = \sqrt{m^2 + p_T^2}; \beta_r(r) = \beta_s \left(\frac{r}{R}\right)^n; \rho = \tanh^{-1} \beta_r$$

The result of these fits done simultaneously on π^+ , K^+ and p spectra, in terms of $T_{\text{kin}} - \langle \beta_T \rangle$ correlation as a function of charged particle multiplicity and comparison with the results obtained for Pb-Pb and p-Pb as a function of centrality and multiplicity classes, respectively, are presented in Fig. 2(a) [1]. One could conclude that for pp collisions at 7 TeV, the $T_{\text{kin}} - \langle \beta_T \rangle$ correlation as a function of charged particle multiplicity has a trend rather similar with the one observed in heavy ion collisions, i.e. the freeze-out kinetic temperature decreases and the average transverse expansion velocity increases with charged particle multiplicity (pp) or increasing centrality (A-A). However, there is a quantitative difference between pp and A-A collisions, i.e. T_{kin} is systematically lower and $\langle \beta_T \rangle$ systematically larger than the pp values, the difference increasing towards higher centralities. Within the error bars, the results for p-Pb at 5.02 TeV are the same with the ones evidenced in pp. Such a correlation is not reproduced by PYTHIA for the pp case. Including the color reconnection mechanism [4] it seems that the model starts to show a similar trend but with values of T_{kin} about 40 MeV lower. On Fig. 2(b) a similar plot [5] is shown, including all energies measured at RHIC [5] and Pb-Pb at 2.76 TeV at LHC [6].

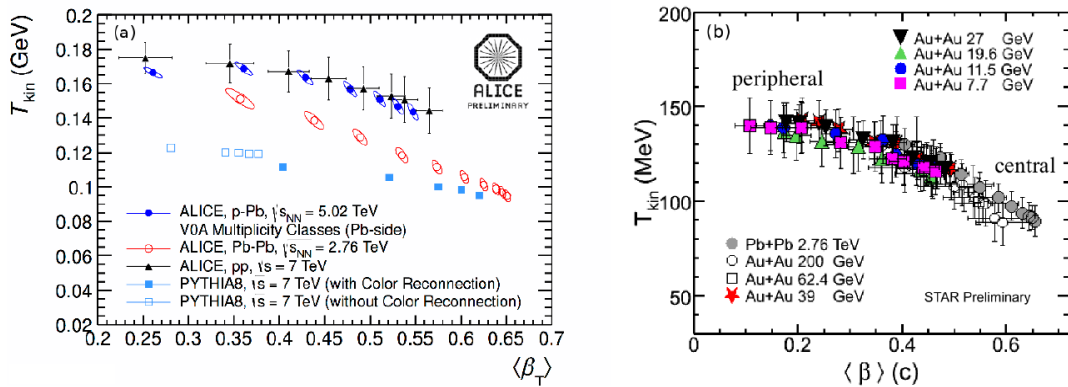


Fig. 2. (a) $T_{\text{kin}} - \langle \beta_T \rangle$ correlation as a function of multiplicity, multiplicity classes and centrality for pp ($\sqrt{s} = 7$ TeV), p-Pb ($\sqrt{s_{\text{NN}}} = 5.02$ TeV) and Pb-Pb ($\sqrt{s_{\text{NN}}} = 2.76$ TeV), respectively [1, 2]; (b) $T_{\text{kin}} - \langle \beta_T \rangle$ correlation as a function of centrality for Au+Au at RHIC energies [5] and Pb-Pb [6].

Another aspect worth to be mentioned is the correlation between the expansion profile (n) and $\langle \beta_T \rangle$. This correlation is presented in Fig. 3(a) [1]. It is clearly seen that all three systems follow exactly the same correlation. Towards the highest multiplicity in the pp case, the expansion velocity becomes linear as a function of position within the fireball. The $n - 1/T_{\text{kin}}$ correlation (Fig. 3(b)) shows that the PYTHIA prediction is completely different than the experimental one.

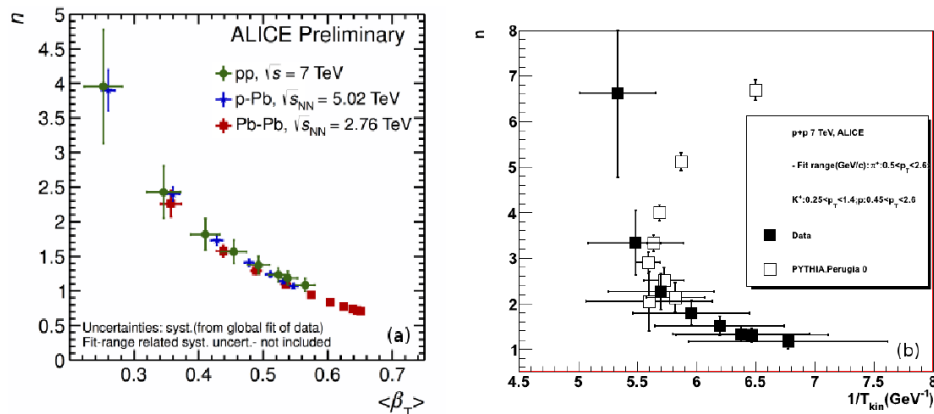


Fig. 3. (a) $n - \langle \beta_T \rangle$ correlation as a function of charged particle multiplicity in pp at 7 TeV and centrality and multiplicity classes in Pb-Pb at 2.76 TeV and p-Pb at 5.02 TeV, respectively [1]; (b) $n - 1/T_{\text{kin}}$ correlation as a function of charged particle multiplicity in pp at 7 TeV; data - full symbols, PYTHIA - open symbols.

- Extension of the kaon p_T distribution range and validation of the Bayesian PID method

In order to test the possibility to extend the p_T range for the kaon distributions we analyzed approximately $19 \cdot 10^6$ inelastic pp collisions collected by ALICE during the 2010 run at the LHC (period LHC10d, pass 2), using a minimum-bias trigger, at an injection energy of $\sqrt{s} = 7$ TeV. The minimum-bias trigger required a signal in one of the two VZERO counters or one of the two layers of the Silicon Pixel Detector (SPD) in addition to the LHC beam crossing signal. The information from the VZERO detectors was used to reject beam-gas and beam-halo collisions. From this sample, we selected events based on the measured charged-particle multiplicity estimated using the combined multiplicity method within the pseudorapidity range $|\eta| < 0.8$. Events were required to have a primary vertex within Δz less than 10 cm from the nominal Interaction Point. The minimum number of clusters associated with the track in the TPC was 70. Tracks having a χ^2/N value of less than 4 for the Kalman fit to the reconstructed position of the TPC clusters were selected, with N being the number of clusters. A p_T -dependent DCA (Distance of Closest Approach) cut of $0.018 + 0.035 \cdot p_T^{-1.01}$ cm in the transverse plane, corresponding to 7σ for pions, and a further cut of 2 cm in the longitudinal direction, were used in order to reduce the contamination from secondary particles produced in the weak decays of strange particles, conversions, and secondary hadronic interactions in the detector material. For this analysis we used a rapidity range of $|y| < 0.5$ in conjunction with the excellent identification capability of ALICE, which is based on a combination of the specific energy loss and momentum measurement by the TPC and the particle velocity measured by the time of flight delivered by the TOF detector.

The efficiency and other correction factors, including acceptance, were estimated run-by-run, using simulated events anchored to the data runs (simulation period LHC10f6a). The simulation was based on the PYTHIA6.4 event generator tune D6T, with events propagated through the detector using GEANT3.

The analysis was performed using AliRoot version vAN-20141013. The tender was used in order to account for the evolutions in the reconstruction. Pile-up events were rejected using the IsPileupFromSPDInMultBins method. The analyzed runs of LHC10d were: 125085, 125101, 125847, 125850, 125855, 126090 and 126097.

Particle identification strategy

The Bayesian PID framework with priors obtained from the data using the iterative procedure, was used for the identification of charged hadrons. The TuneOnData and EtaCorrection options were switched on. The particle species with the highest probability was selected, without applying any purity cut. The performance of the method was cross-checked comparing the p_T spectra with the ones obtained using $n\sigma$ and unfolding techniques.

The identification of charged hadrons is based on the information delivered by the TPC and TOF subdetectors in the ALICE central barrel in different momentum ranges, as shown in Table 1.

Hadron	TPC	TPC-TOF
π^+	$0.2 < p_T < 0.5$	$0.5 < p_T < 2.5$
K^+	$0.3 < p_T < 0.45$	$0.45 < p_T < 2.5$
p	$0.5 < p_T < 0.8$	$0.8 < p_T < 2.5$

Table 1. PID detectors and momentum ranges (GeV/c) used in spectra analysis.

PID efficiency and contamination

The PID efficiencies for the TPC - TOF bayesian particle identification are presented in Fig. 4. The PID efficiency ϵ_{ii} of detecting a species i is defined as the fraction of particles belonging to species i identified correctly over the total number of particles belonging to species i .

The percentage of misidentified particles, at transverse momenta up to 2.5 GeV/c, is below 5% for pions and protons, and it reaches 20% for kaons.

In order to avoid the dependence of the corrections on the model abundances the spectra are corrected for

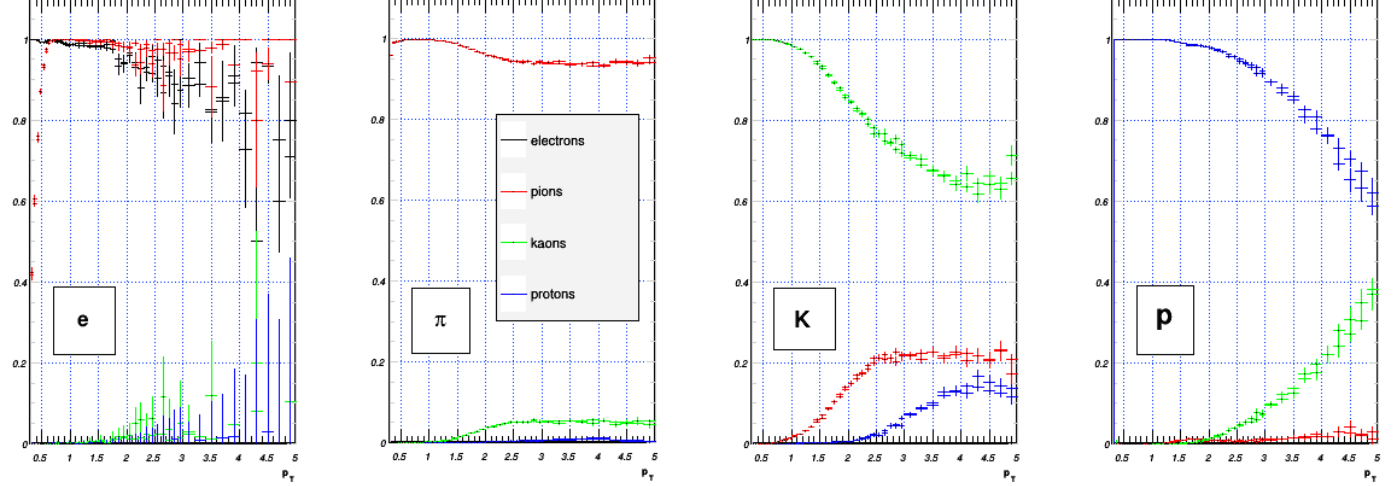


Fig. 4. PID efficiencies and the percentage of misidentified particles for TPC-TOF, from left to right for electrons, pions, kaons and protons.

PID efficiency and for contaminations using the ϵ_{PID} matrix method.

The diagonal elements ($i = j$) of this matrix are the efficiencies ϵ_{ii} defined above, while the non diagonal elements (m_{ij} , $i \neq j$) represent the probability of misidentifying a species i as a different species j . If only pions, kaons and protons are considered, the 3×3 ϵ_{PID} matrix is then defined as:

$$\begin{pmatrix} \epsilon_{\pi\pi} & m_{\pi K} & m_{\pi p} \\ m_{K\pi} & \epsilon_{KK} & m_{Kp} \\ m_{p\pi} & m_{pK} & \epsilon_{pp} \end{pmatrix}$$

In the present analysis, for each p_T bin, a 4×4 matrix is defined (similar with the one described above, but including also the PID efficiency for the electrons), the matrix is inverted, and relation (1) is used in order to obtain the corrected spectra.

$$A_{\text{true}} = (\epsilon_{PID})^{-1} \times A_{\text{meas}} \quad (1)$$

where A_{true} are the true particle abundances and A_{meas} are the measured abundances.

In addition to this, the spectra are corrected by the tracking, matching and main vertex determination efficiencies. The contribution from secondary particles that were not removed by the DCA cut, described in the above subsection, is determined using a data driven method and it is extracted from the final spectra.

Comparison with MB p_T spectra obtained using the $n\sigma$ and unfolding methods

The preliminary spectra in minimum-bias pp data at $\sqrt{s} = 7$ TeV are based on the periods LHC10b and LHC10c.

Since the present study is based on data from LHC10d, it must be ensured that the corrections are the same as those performed in the periods mentioned above. In particular, this must be considered for the correction

of the main vertex in order to account for differences between the data and MC. While the z distribution of the main vertex observed in the data is reproduced quite well in MC for LHC10b and LHC10c, this is not the case for LHC10d. Therefore, a z_{VTX} correction is applied at the global level, i.e. the data are corrected with the ratio of the normalised z distribution of the main vertices, relative to the same quantity corresponding to MC. This is performed within ± 10 cm, which is the range used in this analysis. The resulting correction factor is 1.016.

The final MB p_T distributions from this analysis are compared with the p_T distributions of preliminary 7 TeV pp MB spectra obtained by merging results from the $n\sigma$ method, the unfolding procedure and kinks in Fig. 5. On the upper row of the figure, a very good agreement within the statistical uncertainties (the systematic uncertainties were only considered for the preliminary 7 TeV pp MB spectra) can be observed between the p_T spectra obtained using the two methods. Their ratios, presented in the bottom row, show an agreement within $\pm 5\%$. It must also be noted that this agreement was reached despite differences in the beam conditions between the periods under analysis. The correction for secondary particles is very important. This correction is obtained by fitting the experimental DCA distributions with a sum of weighted MC DCA distributions of primary particles, weak decays and material interactions, the weights being the fit parameters. This rather complex procedure might produce some differences between analyses and brings part of the difference observed, especially at low p_T , where PID for protons is relatively simple, no matter which method is chosen.

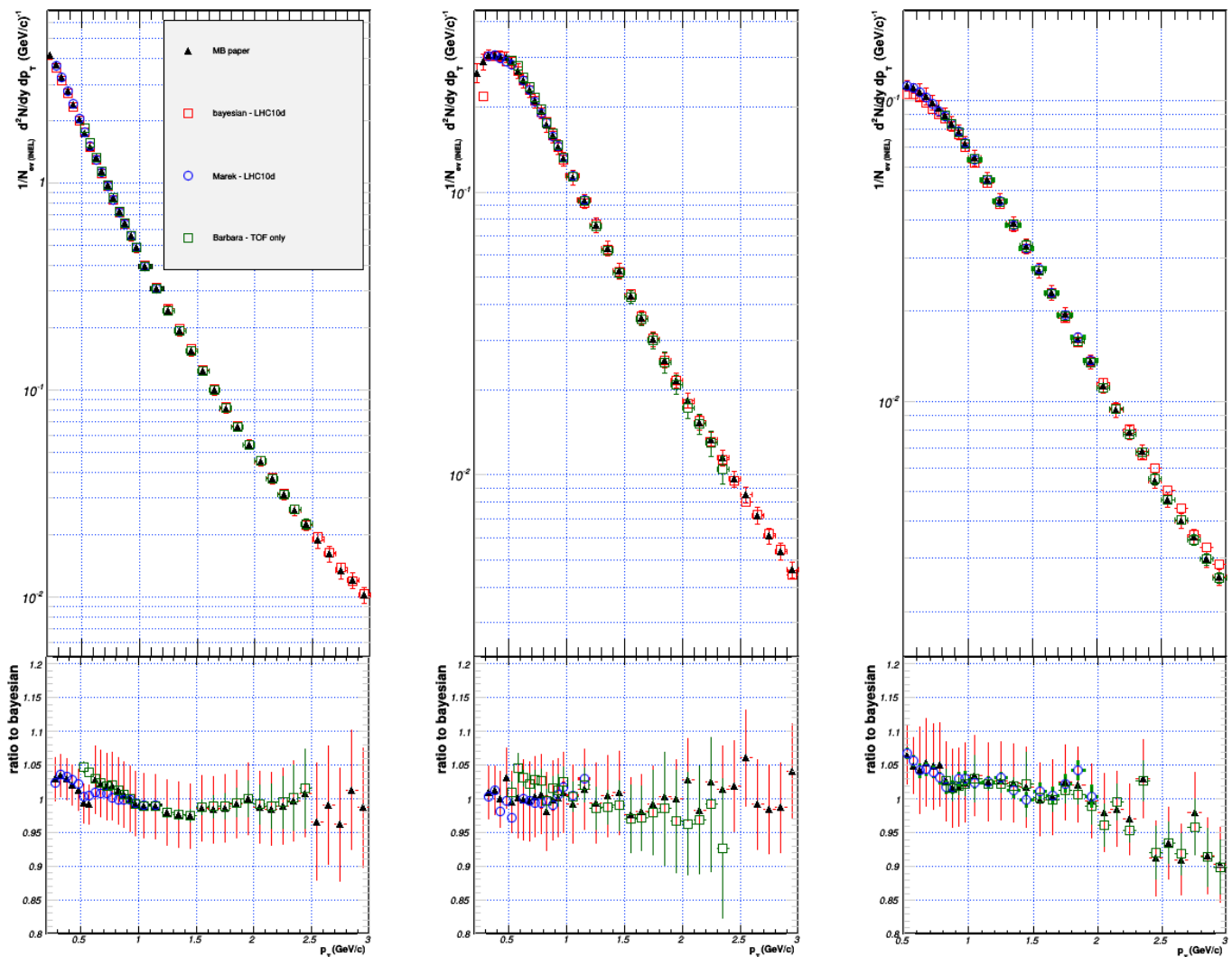


Fig. 5. MB p_T spectra from Bayesian analysis (red squares), compared with the p_T distributions of preliminary MB spectra from pp collisions at 7 TeV (black triangles), TOF only p_T spectra (green squares) and with results obtained using n -sigma method based on TPC (blue circles).

- *Study of Non-Perturbative Particle Production in Strong Fields and Collective Effects*

We continued our studies on the influence of possible strong homogeneous constant SCF on prompt open charm mesons (D^0 , D^+ , D^{*+} , D_s^+) production in Pb - Pb and minimum bias pp collisions in the framework of the HIJING / $B\bar{B}$ v2.0 model. The measured ratios of prompt strange D_s^+ mesons to the non-strange D^0 and D^+ mesons in minimum bias pp collisions at $\sqrt{s} = 7$ TeV help to verify our assumptions and to set by comparison with ALICE data, the strangeness suppression factor for charm mesons (see Fig. 6). We assume an energy and system dependence of the effective string tension, κ , equivalent to an *in-medium mass* modification of charm and strange quark. The effective string tension controls $Q\bar{Q}$ pair creation rates and suppression factors $\gamma_{Q\bar{Q}}$.

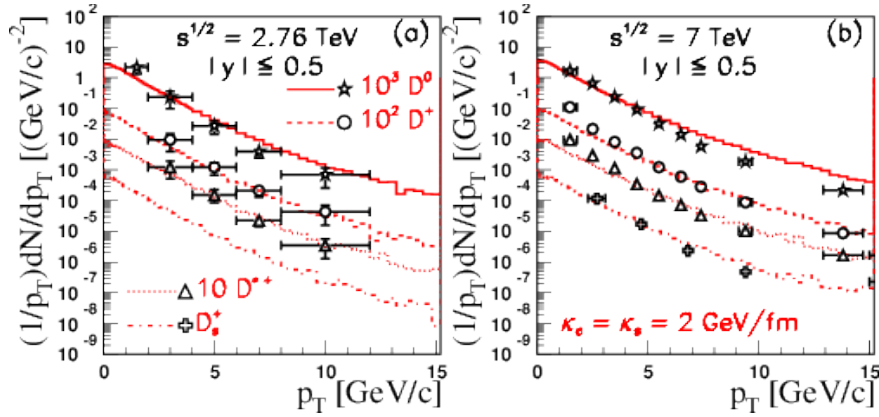


Fig. 6. (Color online) HIJING/ $B\bar{B}$ v2.0 predictions for p_T distributions at mid-rapidity for $p+p \rightarrow (D + \bar{D})/2 + X$ with $D = D^0$ (solid histograms); $D = D^+$ (dashed histogram); $D = D^{*+}$ (dotted histograms); and $D = D_s^+$ (dash-dotted histogram). The results are compared to ALICE data at $\sqrt{s} = 2.76$ TeV (left panel) and at $\sqrt{s} = 7$ TeV (right panel). For clarity, the experimental data and theoretical results are multiplied with a factor indicated in the figure. Only statistical error bars are shown.

For Pb-Pb collisions at $\sqrt{s_{NN}} = 2.76$ TeV all nuclear effects included in the model, *e.g.*, strong color fields, shadowing and quenching should be taken into account. Partonic energy loss and jet quenching process as embedded in the model achieve a reasonable description of the suppression ($R_{pPb}^D < 1$) at moderate and high transverse momentum. Moreover, at low and intermediate p_T ($0 < p_T < 8$ GeV/c) the model predicts a quark mass hierarchy. By computing the nuclear modification factor R_{pPb}^D , we show that the above nuclear effects constitute important dynamical mechanisms that explain better the observed prompt D mesons and charged particles production as observed by the ALICE collaboration [7].

- *Comparison of experimental results for pp collisions at $\sqrt{s} = 7$ TeV with the EPOS model*

EPOS in its initial version was a sophisticated multiple scattering approach based on partons and Pomerons (parton ladders), with special emphasis on high parton densities. The latter aspect, particularly important in proton-nucleus or nucleus-nucleus collisions, is taken care of via an effective treatment of Pomeron-Pomeron interactions, referred to as parton ladder splitting. In addition, collective effects are introduced after separating the high density central core from the peripheral corona. EPOS is the successor of the NEXUS model.

The EPOS3 approach provides within a unique theoretical scheme the initial conditions for a hydrodynamical evolution in p-p, p-A, and HI collisions. The initial conditions are generated in the Gribov-Regge multiple scattering framework. An individual scattering is referred to as Pomeron, identified with a parton ladder, eventually showing up as flux tubes (also called strings). Each parton ladder is composed of a perturbative QCD (pQCD) hard process, plus initial- and final-state linear parton emission. The formalism is referred to as “parton-based Gribov Regge theory” and described in detail in Ref. [8]. Based on these initial conditions, ideal hydrodynamical calculations to analyze HI and p-p scattering at the BNL Relativistic Heavy Ion Collider (RHIC) and CERN Large Hadron Collider (LHC) have been performed. In [9] two

major improvements: a more sophisticated treatment of nonlinear effects in the parton evolution by considering individual (per Pomeron) saturation scales and a 3D + 1 viscous hydrodynamical evolution were implemented. There are also changes in the core-corona procedure, which amounts to separation of the initial energy of the flux tubes into a part which constitutes the initial conditions for hydro (core) and the particles which leave the “matter.” This is crucial in all collision types.

As a consequence of the rescaling due to collective flows, and in particular the radial flow, the number of secondary particles produced by the clusters is reduced. In case of a consistent treatment of cross-section and particle production like in EPOS, this property is needed in the case of HI collisions where less particles are observed than produced by the model without final state interactions. And indeed a proper hydro treatment like in EPOS 2 or 3 requires a large multiplicity in the initial state to finish with the correct multiplicity after a long evolution of the large volume of the core. But in the case of light system, like pp, using EPOS 2 or 3 with a realistic treatment of the hydrodynamical evolution with proper hadronization such an effect was not observed. In that case the large flow comes from the quick expansion of the very small volume of the core. As a consequence, in EPOS LHC [10] a different type of radial flow in case of very dense system in a small volume (where the critical energy density is reached because of multiple scattering between partons in a single pair of nucleons like in pp) was introduced. For this pp flow, characterized by the maximal radial rapidity y_{rad} , the mass of the cluster M is not changed before hadronization (multiplicity is conserved) but the energy conservation is imposed by a simple rescaling of the total momentum P (larger p_T are compensated by smaller p_z) after the radial boost. Of course a smooth transition is needed between the two kinds of system and the transition is observed in p-A interactions.

EPOS LHC and EPOS3 codes have been implemented in our group. The p_T distributions for pions, kaons and protons in pp collisions at $\sqrt{s} = 7$ TeV have been compared with both versions of the models for MB and all the multiplicity bins. An example of this comparison can be followed in Fig. 7. As a conclusion the EPOS LHC version provides a slightly better overall description of the data as compared to EPOS3 version. Nevertheless, very accurate final experimental distributions which will be obtained by us and the comparison with theoretical predictions will contribute to the refinement of the EPOS3 model based on hydrodynamical calculations and to the answer of the question: Do we see collective radial flow in pp collisions at LHC?

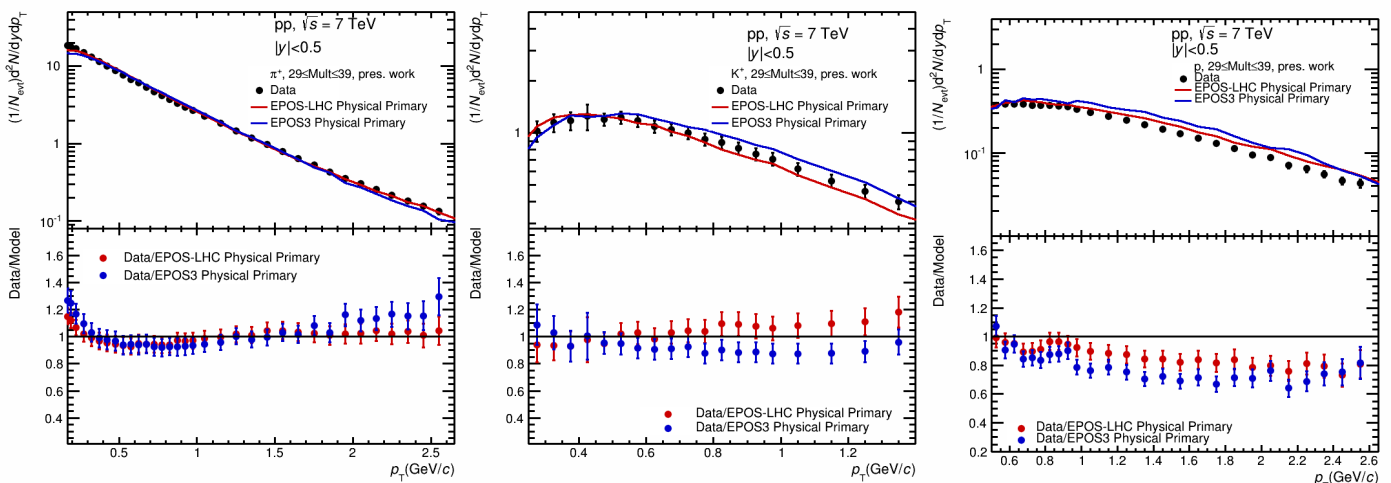


Fig. 7. Comparison of the experimental data for p_T distributions of pions, kaons and protons in pp collisions at $\sqrt{s} = 7$ TeV, with the EPOS LHC and EPOS3 calculations for one multiplicity bin.

In the year 2014 our group was co-author to 18 ISI papers and over 20 oral presentations at different international conferences and had 7 presentations in Spectra group, PWG-LF, Physics Forum of the ALICE Collaboration, one oral presentation at Quark Matter 2014 (in press in Nucl. Phys. A), one invited lecture at the Carpathian Summer School, Sinaia, July 2014 (to appear in AIP Conference Proceedings) and one paper in Jour. Phys. G.

References

1. ALICE Collaboration, C. Andrei et al. Nucl. Phys. A 20024, S0375-9474(14)00251-6:10.1016/j.nuclphysa.2014.08.002, Quark Matter 2014.
2. ALICE Collaboration, B. Abelev et al. Phys. Lett. B, 728:25, 2014.
3. E. Schnedermann et al. Phys. Rev. C, 48:2462, 1993.
4. R. Corke and T. Sjostrand. JHEP, 1001:35, 2010.
5. STAR Collaboration, L. Kumar, Quark Matter 2014.
6. ALICE Collaboration, B. Abelev et al. Phys. Rev. C, 88:044910, 2013.
7. V. Topor Pop, M. Gyulassy, J. Barrette, C. Gale and M. Petrovici, Jour. Phys. G 41:115101, 2014.
8. H. J. Drescher et al., Phys. Rep. 350:93, 2001.
9. K. Werner, B. Guiot, Yu. Karpenko, T. Pierog, Phys. Rev. C 89:064903, 2014.
10. T. Pierog et al., arXiv:1306.0121v2 [hep-ph] (2013) DESY-13-125.

Director proiect,

Prof. Dr. Mihai Petrovici